CrystEngComm

Accepted Manuscript

ROYAL SOCIETY OF CHEMISTRY

www.rsc.org/crystengcomm

Journal Name

ARTICLE

Vanadoantimonates: from discrete clusters to high dimensional aggregates

Received 00th January 20xx,
Accepted 00th January 20xx

DOI: 10.1039/x0xx00000x

www.rsc.org/

Hai-Yang Guo,[a] Xiao Zhang[b,c]* Xiao-Bing Cui[a]* Qi-Sheng Huo[a]and Ji-Qing Xu[a]

Five new vanadoantimonates $[Cd(en)_3]_3[Sb_6V_{15}O_{42}(H_2O)]\cdot 8H_2O$ (**1**), $[Ni(en)_3]_2[H_2Sb_6V_{15}O_{42}(H_2O)]\cdot 5H_2O$ (**2**), $[Co(en)_3]_2[H_2Sb_6V_{15}O_{42}(H_2O)]\cdot 5H_2O$ (**3**), $[H_4Sb_8V_{14}O_{42}(H_2O)]\cdot 5H_2O$ (**4**) and $[Co(enMe)_3]_2[Sb_8V_{14}O_{42}(H_2O)]\cdot 4H_2O$ (**5**) (en= Ethylenediamine, enMe=1,2- propanediamine) have been obtained under hydrothermal conditions and characterized by IR, UV-Vis, XRD, ESR and CD spectra. Compound **1** is a chiral compound constructed from $[Sb_6V_{15}O_{42}(H_2O)]^{6-}$ (Sb_6V_{15}) and $[Cd(en)_3]^{2+}$. Compounds **2** and **3** are isostructural and isomorphous. Both compounds are chiral, each of which contains a 2-D inorganic layer formed by $[H_2Sb_6V_{15}O_{42}(H_2O)]^{4-}$ via V-O···Sb contacts. Compound **4** contains a 2-D inorganic layer formed by $[H_4Sb_8V_{14}O_{42}(H_2O)]$, of which $[H_4Sb_8V_{14}O_{42}(H_2O)]$ is directed by both V-O···Sb and Sb-O···Sb interactions. Compound **5** contains a 1-D zigzag chain structure formed by $[Sb_8V_{14}O_{42}(H_2O)]^{4-}$ (Sb_8V_{14}) via Sb-O···Sb contacts.

Introduction

Polyoxometalates (POMs) form a distinctive class of inorganic metal-oxygen cluster compounds of electronic versatility and structural variation, with impacts ranging from catalysis, analysis, biochemistry, materials science and medicine.[1] Though the class of POMs has been known for almost 200 year,[2] it continues to be a focus in the ongoing research because of the gradual and progressive development of POM structures and their properties. Many of fundamental properties of POM that have impact on its applications, including elemental composition, solubility, redox potential(s), charge density, size, and shape, can be systematically altered to a considerable degree.[3]

An important subclass of POMs is the family of arsenic-vanadium clusters derived from the well-known $\{V_{18}O_{42}\}$ cluster, which display interesting electronic and magnetic properties.[4] Our group has focused on the synthesis of vanadoarsenates for several years and has synthesized a series of organic-inorganic hybrids constructed from vanadoarsenates and transition metal complexes (TMCs).[5] In addition, we also began to synthesize compounds based on antimony, which belongs to the same main group to arsenic and we think perhaps similar compounds can be obtained. Moreover, several properties of vanadoantimonates are promising for different potential applications like in sorption,[6] selective oxidation reactions,[7] and as $deNO_x$ catalysts[8] or heterogeneous oxidation catalysts.[9] Further investigations have shown that the antimony cations have a stabilizing effect on polyoxometalates at high temperatures.[10] Unfortunately, the preparation of antimony analogues was not easy. After several years, we only obtained two antimony analogues.[11]

Meanwhile, other researchers, especially Bensch et al. also focused on the study of vanadoantimonates, and a series of vanadoantimonates were successfully synthesized.[12] Recently, Monakhov, Bensch and Kögerler published a milestone review about derivatives of polyoxovanadates,[13] in which syntheses and structures of vanadoarsenates, vanadoantimonates and vanadogermanates etc. were carefully reviewed. Vanadoantimonates can significantly expand the area of polyoxovanadate chemistry due to the introduction of a different functionality compared to the As-containing congeners.[12f]

However, we must point out that it is still a great challenge for chemists to synthesize new vanadoantimonates. Compared with vanadoarsenates, the number of vanadoantimonates is still far too small. Perhaps the reason can be ascribed to the inertness of antimony and the instability of the crystals of vanadoantimonates. Recently, we want to further the study of vanadoantimonates, and fortunately, we successfully synthesized five new vanadoantimonates $[Cd(en)_3]_3[Sb_6V_{15}O_{42}(H_2O)]\cdot 8H_2O$ (**1**), $[Ni(en)_3]_2[H_2Sb_6V_{15}O_{42}(H_2O)]\cdot 5H_2O$ (**2**), $[Co(en)_3]_2[H_2Sb_6V_{15}O_{42}(H_2O)]\cdot 5H_2O$ (**3**), $[H_4Sb_8V_{14}O_{42}(H_2O)]\cdot 5H_2O$ (**4**) and $[Co(enMe)_3]_2[Sb_8V_{14}O_{42}(H_2O)]\cdot 4H_2O$ (**5**). Compound **1** is a chiral compound constructed from $[Sb_6V_{15}O_{42}(H_2O)]^{6-}$ and $[Cd(en)_3]^{2+}$

[a] College of Chemistry and State Key Laboratory of Inorganic Synthesis and Preparative Chemistry, Jilin University, Changchun, Jilin, 130023. E-mail: cuixb@mail.jlu.edu.cn.
[b] MIIT Key Laboratory of Critical Materials Technology for New Energy Conversion and Storage, School of Chemistry and Chemical Engineering, Harbin Institute of Technology, Harbin, P.R. China, 150080
[c] Key Laboratory of Functional Inorganic Material Chemistry, Ministry of Education, School of Chemistry and Materials Science, Heilongjiang University, Harbin 150080, People's Republic of China.
† Footnotes relating to the title and/or authors should appear here.
Electronic Supplementary Information (ESI) available: [details of any supplementary information available should be included here]. See DOI: 10.1039/x0xx00000x

having two different screw configurations. Compounds **2** and **3** are isostructural and isomorphous. Both compounds are chiral, each of which is formed by $[H_2Sb_6V_{15}O_{42}(H_2O)]^{4-}$ and $[M(en)_3]^{2+}$ (M=Ni for **2** and Co for **3**) having two different screw configurations. Compounds **2** and **3** also contain 2-D inorganic layers formed by $[Sb_6V_{15}O_{42}(H_2O)]^{6-}$ via V-O···Sb contacts. Compound **4** contains a 2-D inorganic layer formed by $[H_4Sb_8V_{14}O_{42}(H_2O)]$, of which $[H_4Sb_8V_{14}O_{42}(H_2O)]$ is directed by both V-O···Sb contacts and Sb-O···Sb interactions. Compound **5** contains a 1-D zigzag chain structure formed by $[Sb_8V_{14}O_{42}(H_2O)]^{4-}$ via Sb-O···Sb contacts.

Experimental

Materials and measurements

All the chemicals used were of reagent grade without further purification. C, H, N elemental analyses were carried out on a Perkin-Elmer 2400 CHN elemental Analyzer. Inductively coupled plasma (ICP) elemental analyses were carried out on a Perkin-Elmer Optima 3300DV ICP spectrometer. Infrared spectra were recorded as KBr pellets on a Perkin-Elmer SPECTRUM ONE FTIR spectrophotometer. UV-vis spectra were recorded on a Shimadzu UV-3100 spectrophotometer. Powder XRD patterns were obtained with a Scintag X1 powder diffractometer system using Cu Kα radiation with a variable divergent slit and a solid-state detector. Electron spin resonance (ESR) spectra were performed on a JEOL JES-FA200 spectrometer operating in the X-band mode. The g value was calculated by comparison with the spectrum of 1,1-diphenyl-2-picrylhydrazyl (DPPH), whereas the spin concentrations were determined by comparing the recorded spectra with that of a Mn marker and DPPH, using the built-in software of the spectrometer. Solid state circular dichroism (CD) spectra were recorded at room temperature with a Jasco J-810(S) spectropolarimeter.

Synthetic procedures

Synthesis of $[Cd(en)_3]_3[Sb_6V_{15}O_{42}(H_2O)]\cdot 8H_2O$ (1) Sb_2O_3 (0.6g, 3mmol), NH_4VO_3 (0.6g, 5mmol), en (2ml) and H_2O (2ml) was mixed and stirred for 3h, then $CdCl_2$ (0.183g, 1mmol) was added, the resulting suspension was further stirred for 1h, the pH of the mixture was 10. The mixture was sealed in a Teflon-lined stainless bomb and heated at 170°C for 5 days under autogenous pressure and then left to cool to room temperature. The resulting black bulk crystals of **1** were filtered off, washed with water and air-dried at room temperature (ca, 46.0% yield based on V). Calcd. For $C_{18}H_{90}Cd_3N_{18}O_{51}Sb_6V_{15}$: Sb, 22.78; Cd, 10.52; V, 23.83; C, 6.74; H, 2.83; N, 7.86%. Found: Sb, 22.34; Cd, 10.70; V, 23.55; C, 6.44; H, 2.43; N, 7.76%.

Synthesis of $[Ni(en)_3]_2[H_2Sb_6V_{15}O_{42}(H_2O)]\cdot 5H_2O$ (2) Sb_2O_3 (0.6g, 3mmol), NH_4VO_3 (0.6g, 5mmol), en (2ml), DMF (2ml, DMF= N,N-Dimethylformamide) and H_2O (2ml) was mixed and stirred for 3h, then $Ni(NO_3)_2\cdot 6H_2O$ (0.291g, 1mmol) and TPABr (0.266, 1mmol, TPABr= Tetrapropylammonium bromide) were added, the resulting suspension was further stirred for 1h, the pH of the mixture was 8.5. The mixture was sealed in a Teflon-lined stainless bomb and heated at 170°C for 5 days under autogenous pressure and then left to cool to room temperature. The resulting black polyhedron crystals of **2** were filtered off, washed with water and air-dried at room temperature (ca, 58.2% yield based on V). Calcd. For $C_{12}H_{62}N_{12}Ni_2O_{48}Sb_6V_{15}$: Sb, 26.52; Ni, 4.26; V, 27.74; C, 5.23; H, 2.27; N, 6.10%. Found: Sb, 26.47; Cd, 4.19; V, 27.42; C, 5.20; H, 2.09; N, 6.16%.

Synthesis of $[Co(en)_3]_2[H_2Sb_6V_{15}O_{42}(H_2O)]\cdot 5H_2O$ (3) Sb_2O_3 (0.6g, 3mmol), NH_4VO_3 (0.6g, 5mmol), en (2ml), DMF (2ml) and H_2O (2ml) was mixed and stirred for 3h, then $Co(NO_3)_2\cdot 6H_2O$ (0.291g, 1mmol) and TEAB (0.266g, 1mmol, TEAB= Tetraethylammonium bromide) were added, the resulting suspension was further stirred for 1h, the pH of the mixture was 9.0. The mixture was sealed in a Teflon-lined stainless bomb and heated at 170°C for 5 days under autogenous pressure and then left to cool to room temperature. The resulting black polyhedron crystals of **3** were filtered off, washed with water and air-dried at room temperature (ca, 62.0% yield based on V). Calcd. For $C_{12}H_{62}Co_2N_{12}O_{48}Sb_6V_{15}$: Sb, 26.52; Co, 4.28; V, 27.73; C, 5.23; H, 2.27; N, 6.10%. Found: Sb, 26.41; Co, 4.15; V, 27.55; C, 5.11; H, 2.13; N, 6.02%.

Synthesis of $[H_4Sb_8V_{14}O_{42}(H_2O)]\cdot 5H_2O$ (4) Sb_2O_3 (0.6g, 3mmol), NH_4VO_3 (0.6g, 5mmol), $Cu(Ac)_2\cdot H_2O$ (0.323g, 1.6mmol), Piperazine (0.582g, 3mmol), 2,2'-bpy (0.306g, 2mmol), DMF (2ml) and H_2O (2ml) was mixed and stirred for 3h, the pH of the mixture was 8.0. The mixture was sealed in a Teflon-lined stainless bomb and heated at 170°C for 5 days under autogenous pressure and then left to cool to room temperature. The resulting black polyhedron crystals of **4** were filtered off, washed with water and air-dried at room temperature (ca, 54.2% yield based on V). Calcd. For $H_{16}O_{48}Sb_8V_{14}$: Sb, 39.41; V, 28.86%. Found: Sb, 39.29; V, 28.75%. $Cu(Ac)_2\cdot H_2O$, piperazine and 2,2'-bpy are required for the synthesis of compound **4**, though they are absent in the product. Such a phenomenon is not unusual in the hydrothermal synthesis.[14] The identical experimental procedure only without the addition of piperazine has been done, no crystals were obtained. The identical procedure except that $Cu(Ac)_2\cdot H_2O$ was not added and 2,2'-bpy was replaced by en has also been done, no crystals were obtained too.

Synthesis of $[Co(enMe)_3]_2[Sb_8V_{14}O_{42}(H_2O)]\cdot 4H_2O$ (5) $CoSO_4\cdot 7H_2O$ (0.281g, 1mmol), enMe (2ml), DMF (2ml) and H_2O (2ml) was mixed and stirred for 1h, Sb_2O_3 (0.6g, 3mmol) and NH_4VO_3 (0.6g, 5mmol) was added, the resulting suspension was further stirred for 2h, the pH of the mixture was 10.0. The mixture was sealed in a Teflon-lined stainless bomb and heated at 170°C for 5 days under autogenous pressure and then left to cool to room temperature. The resulting black polyhedron crystals of **5** were filtered off, washed with water and air-dried at room temperature (ca, 58.3% yield based on V). Calcd. For $C_{18}H_{70}Co_2N_{12}O_{47}Sb_8V_{14}$: Sb, 32.34; Co, 3.91; V, 23.68; C, 7.18; H, 2.34; N, 5.58%. Found: Sb, 32.22; Co, 3.85; V, 23.56; C, 7.10; H, 2.18; N, 5.62%.

X-ray crystallography

Table 1. Crystal data and structural refinements for compounds **1** -**5**.

	Compound **1**	Compound **2**	Compound **3**	Compound **4**	Compound **5**
Empirical formula	$C_{18}H_{90}Cd_3N_{18}O_{51}Sb_6V_{15}$	$C_{12}H_{62}N_{12}Ni_2O_{48}Sb_6V_{15}$	$C_{12}H_{62}N_{12}Co_2O_{48}Sb_6V_{15}$	$H_{16}O_{48}Sb_8V_{14}$	$C_{18}H_{70}Co_2N_{12}O_{47}Sb_8V_{14}$
Formula weight	3206.87	2754.75	2755.19	2471.29	3011.88
Crystal system	Monoclinic,	Trigonal	Trigonal	Monoclinic	Monoclini
space group	C 2	R 3	R 3	P $2_1/n$	C 2/*c*
a (Å)	18.188(4)	12.4887(7)	12.454(2)	13.677(1)	29.050(6)
b (Å)	22.992(5)	12.4887(7)	12.454(2)	11.9042(5)	15.812(3)
c (Å)	14.357(3)	39.986(5)	39.916(8)	19.276(2)	21.821(4)
α (˚)	90	90	90	90	90
β (˚)	125.36(3)	90	90	109.348(9)	128.43(3)
γ (˚)	90	120	120	90	90
Volume (Å^3)	4896(2)	5401.0(9)	5361.9(19)	2961.0(4)	7852(4)
Z	2	3	3	2	4
D_C (Mg·m^{-3})	2.175	2.541	2.560	2.772	2.548
μ (mm^{-1})	3.698	4.656	4.628	5.764	4.778
F(000)	3054	3927	3921	2260	5688
ϑ for data collection	2.99 to 27.48	2.14 to 28.29	3.06 to 27.48	3.16 to 29.19	3.12 to 27.48
Reflections collected	24039	17120	17328	16739	35205
Reflections unique	10856	5859	5447	6841	8977
R(int)	0.111	0.1301	0.0582	0.0383	0.0383
Completeness to θ	99.8	99.9	99.8	99.8	99.8
parameters	513	286	287	334	458
GOF on F^2	1.022	1.076	1.038	1.021	1.080
R^a [$I>2\sigma(I)$]	R_1 = 0.0830	R_1 = 0.0890	R_1 = 0.0501	R_1 = 0.0676	R_1 = 0.0405
R^b (all data)	ωR_2 = 0.2305	ωR_2 = 0.2432	ωR_2 = 0.1415	ωR_2 = 0.2071	ωR_2 = 0.0988
Absolute structure parameter	0.11(9)	0.26(11)	0.44(7)		

[a] $R_1 = \sum||F_0|-|F_c||/\sum|F_0|$. [b] $\omega R_2 = \{\sum[w(F_0^2-F_c^2)^2]/\sum[w(F_0^2)^2]\}^{1/2}$.

The reflection intensity data for compounds **1**, **3** and **5** were measured on a Rigaku R-AXIS RAPID diffractometer with graphite monochromated Mo K_α (λ = 0.71073Å) radiation. The reflection intensity data for compounds **2** were measured on a Bruker Apex II diffractometer with graphite monochromated Mo K_α (λ = 0.71073Å) radiation, and the reflection intensity data for compound **4** were measured on an Agilent Technology SuperNova Eos Dual system with a Mo-K_α (λ = 0.71073Å) microfocus source and focusing multilayer mirror optics. None of the crystals showed evidence of crystal decay during data collections. Refinements were carried out with SHELXS-2014/7[15] and SHELXL-2014/7[15] using WinGX via the full matrix least-squares on F^2 method.[16] In the final refinements, all atoms were refined anisotropically in compounds **1**-**5**. The hydrogen atoms of en and enMe ligands in the five compounds were placed in calculated positions and included in the structure factor calculations but not refined. In these heavy-atom structures with reflection data from poor-quality crystals it was not possible to see clear electron-density peaks in difference maps which would correspond with acceptable locations for the various H atoms bonded to water oxygen atoms. The refinements were then completed with no allowance for these water H atoms in the models; water oxygen atoms in compounds **1**, **3** and **4** were also restrained to isotropic behaviours. A summary of the crystallographic data and structure refinements for compounds **1**-**5** is given in Table 1. CCDC number: 1468900 for 1, 1468901 for 2, 1468902 for 3, 1468903 for 4 and 1468904 for 5. These data can be obtained free of charge from The Cambridge Crystallographic Data Centre via www.ccdc.cam.ac.uk/data_request/cif.

Results and discussion

Structure of compound 1

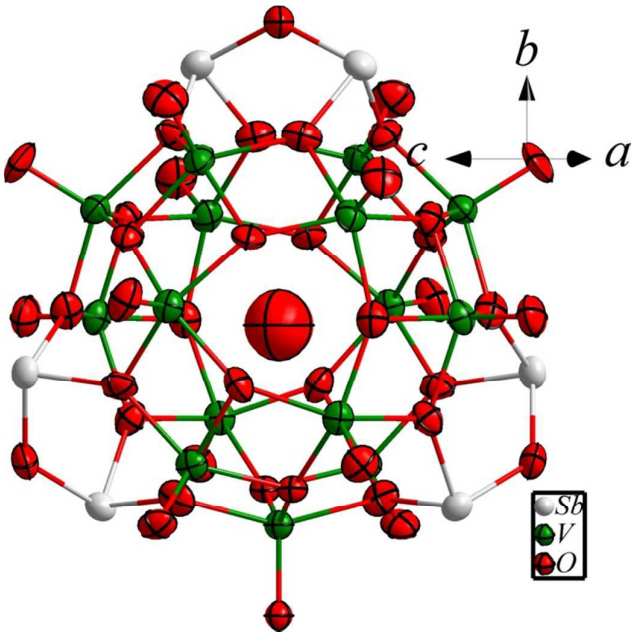

Fig. 1 Ellipsoid representation (50% probability) of the $[Sb_6V_{15}O_{42}(H_2O)]^{6-}$ in compound **1**.

Single-crystal X-ray diffraction analysis reveals that $[Sb_6V_{15}O_{42}(H_2O)]^{6-}$ in compound **1** consists of 15 distorted VO_5 square pyramids and 6 SbO_3 triangular units, with a H_2O enclosed at its center (Fig. 1). $[Sb_6V_{15}O_{42}(H_2O)]^{6-}$ in compound **1** is almost identical to As_6V_{15} reported previously by A. Müller et al.[4a] with all the As atoms replaced by Sb atoms. Bond valence sum calculations suggest that the antimony and vanadium atoms are respectively in +3 and +4 oxidation states.[17]

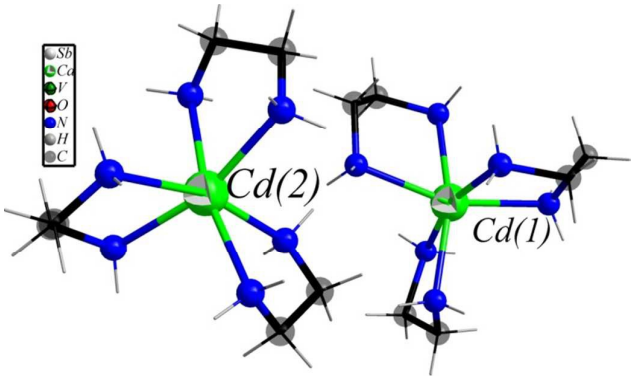

Fig. 2 Ball-and-stick and wire representation of the Cd(1) complex with the right handed screw (Δ) configuration and the Cd(2) complex with the left handed screw (Λ) configuration.

Compound **1** crystallizes in monoclinic space group C2 with V(7), O(5), O(1) and O(5w) on one 2-fold rotation axis, Cd(2) on the other 2-fold rotation axis and all other atoms on general positions. The asymmetric unit contains half a $[Sb_6V_{15}O_{42}(H_2O)]^{6-}$, one and a half of $[Cd(en)_3]^{2+}$ and three and two halves of lattice water molecules. Cd(1) is six-coordinated by six nitrogens from three en ligands, generating a distorted irregular octahedral geometry (Fig. 2). Cd(2), sitting on a 2-fold rotation axis with occupancy factor 0f 0.5, adopts a similar irregular octahedral geometry to that of Cd(1), in which Cd(2) is six-coordinated by six nitrogens from three en ligands too. Cd-N distances are in the range of 2.29(2)-2.43(4)Å. However, detailed analysis found that both complexes are chiral: $[Cd(1)(en)_3]^{2+}$ has the right handed screw (Δ) configuration, but $[Cd(2)(en)_3]^{2+}$ has the left handed screw (Λ) configuration. The distance of the two cadmium centers of the two complexes is 8.322(2)Å.

It should be noted that there are one independent Cd(1), but only half an independent Cd(2) in the asymmetric unit. That is to say, the number of the right handed screw (Δ) configuration $[Cd(1)(en)_3]^{2+}$ is twice of that of the left handed screw (Λ) configuration $[Cd(2)(en)_3]^{2+}$. Therefore, compound **1** is not a meso-compound, but a chiral compound. The single crystal analysis further demonstrated that compound **1** crystalizes in a chiral space group C2.

Structures of compounds 2 and 3

Compounds **2** and **3** are isomorphous and isostructural, hence only compound **2** was described in detail below. Single-crystal X-ray diffraction analysis reveals that $[H_2Sb_6V_{15}O_{42}(H_2O)]^{4-}$ in compound **2** is almost the same as $[Sb_6V_{15}O_{42}(H_2O)]^{6-}$ in compound **1** with two extra hydrogens attached on the surface of the cluster and slight differences in bond lengths and angles. Bond valence sum calculations suggest that the antimony and vanadium atoms are respectively in +3 and +4 oxidation states.[17]

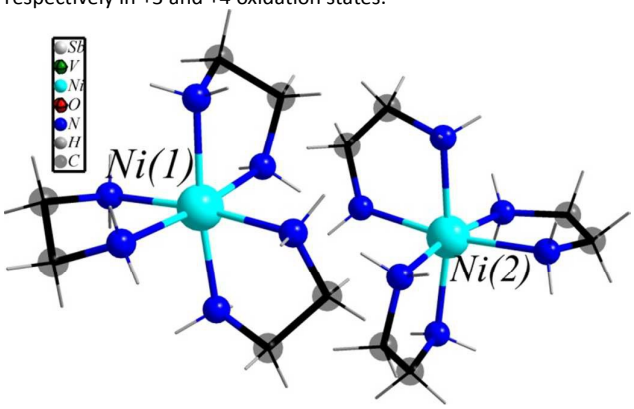

Fig. 3 Ball-and-stick and wire representation of the Ni(1) complex with right handed screw (Δ) configuration and the Ni(2) complex with the left handed screw (Λ) configuration.

Compound **2** crystallizes in trigonal space group R3 with Ni(2), O(1w) and O(3w) on one 3-fold rotation axis, Ni(1) on another 3-fold rotation axis, O(5w) on the third 3-fold rotation axis and all other atoms on general positions. The asymmetric unit contains one third of a $[H_2Sb_6V_{15}O_{42}(H_2O)]^{4-}$, two one-thirds of $[Ni(en)_3]^{2+}$ and one and two one-thirds of lattice water molecules. Both Ni(1) and Ni(2), occupying at special positions with an occupancy factor of 1/3, adopt a six-coordinated octahedral geometry with six nitrogens from three en ligands with Ni-N distances of 2.12(2)-2.16(3)Å (Fig. 3). Similar to the two cadmium complexes in compound **1**, $[Ni(1)(en)_3]^{2+}$ has the right handed screw (Δ) configuration, but $[Ni(2)(en)_3]^{2+}$ has the left handed screw (Λ) configuration. In marked contrast to the two cadmium complexes in compound **1**, the numbers of the two nickel complexes in compound **2** are the same. However, compound **2** also crystalizes in a chiral space group R3.

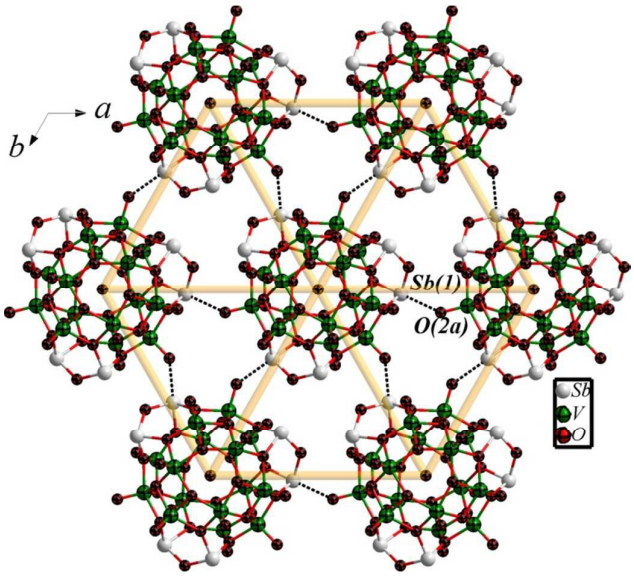

Fig. 4 The 2-D layer structure along the *ab* plane in compound **2**. Symmetry code: a, 1-x, x-y, z.

An unusual feature of compound **2** is that $[H_2Sb_6V_{15}O_{42}(H_2O)]^{4-}$ interacts with six neighboring $[H_2Sb_6V_{15}O_{42}(H_2O)]^{4-}$ in a hexagonal symmetry via V-O···Sb contacts with a Sb···O distance of 2.7745(1)Å into a novel 2-D layer structure along the *ab* plane, as shown in Fig. 4. It should be noted that the centroid-centroid distance of each two $[H_2Sb_6V_{15}O_{42}(H_2O)]^{4-}$ in the layer is identical with a distance of 12.4887(5)Å. Another unusual feature of compound **2** is the arrangement of inorganic layers and nickel complexes. Nickel complexes are sandwiched by two layers of $[H_2Sb_6V_{15}O_{42}(H_2O)]^{4-}$ into a novel 3-D supramolecular structure. There are complex N-H···O hydrogen bonding interactions between nitrogens of nickel complexes and oxygens from $[H_2Sb_6V_{15}O_{42}(H_2O)]^{4-}$ and lattice water molecules with N···O distances of 2.9704(2)-3.1069(2)Å, also there are complex O-H···O hydrogen bonds between lattice water molecules and oxygens of $[H_2Sb_6V_{15}O_{42}(H_2O)]^{4-}$ with O···O distances of 2.7959(2)-3.0354(1)Å (Table s1). These complex synergistic interactions direct POMs and TMCs into the novel 3-D structure.

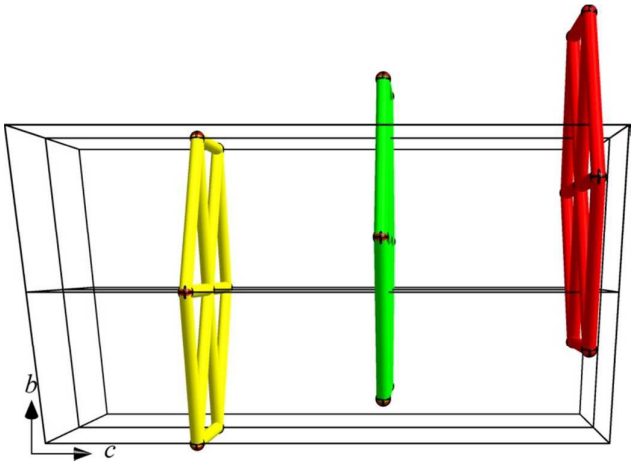

Fig. 5 The arrangement of the three inorganic layers in a unit cell of compound **2**.

The most unusual feature of compound **2** is the arrangement of the inorganic layers. It should be noted that the layers are arranged to be parallel to each other along the *c* axis with the interplane distance of about 13.33Å. That is to say, there are three identical inorganic layers crosscutting each unit cell of the structure of compound **2**, and the three constitute the repeating unit of compound **2**. It should be noted that the three layers are related by the glide plane symmetry, as shown in Fig. 5.

Structure of compound 4

Single-crystal X-ray diffraction analysis reveals that the cluster $[H_4Sb_8V_{14}O_{42}(H_2O)]$ in compound **4** is almost identical to $[Sb_8V_{14}O_{42}(H_2O)]^{4-}$ reported by our group previously[11a] with four extra hydrogens attached on the surface of the cluster and slight differences in bond lengths and angles. Bond valence sum calculations suggest that the antimony and vanadium atoms are respectively in +3 and +4 oxidation states.[17]

Compound **4** crystallizes in monoclinic space group $P2_1/n$ with all atoms located on general positions. The asymmetric unit is composed of half a $[H_4Sb_8V_{14}O_{42}(H_2O)]$ and one and three halves of lattice water molecules. $[H_4Sb_8V_{14}O_{42}(H_2O)]$ in compound **4** is not a discrete one but interacts with neighboring $[H_4Sb_8V_{14}O_{42}(H_2O)]$ via two V-O···Sb interactions with Sb···O distances of 2.7388(1)-2.8883(2)Å or two Sb-O···Sb contacts with a Sb···O distance of 2.8454(1)Å into a novel 2-D layer structure along the *ac* plane. The 2-D layer in compound **4** has some fatal differences from that of compound **2**. Firstly, the 2-D layer in compound **2** is formed by Sb_6V_{15} but the 2-D layer in compound **4** is constructed from Sb_8V_{14}. Secondly and most importantly, each two Sb_8V_{14} are linked to each other via both double V-O···Sb or double Sb-O···Sb contacts in compound **4** but each two Sb_6V_{15} are only joined via one V-O···Sb contact in compound **2**. Thirdly, each two layers in compound **2** sandwiches nickel complexes but each two layers in compound **4** only sandwiches water molecules.

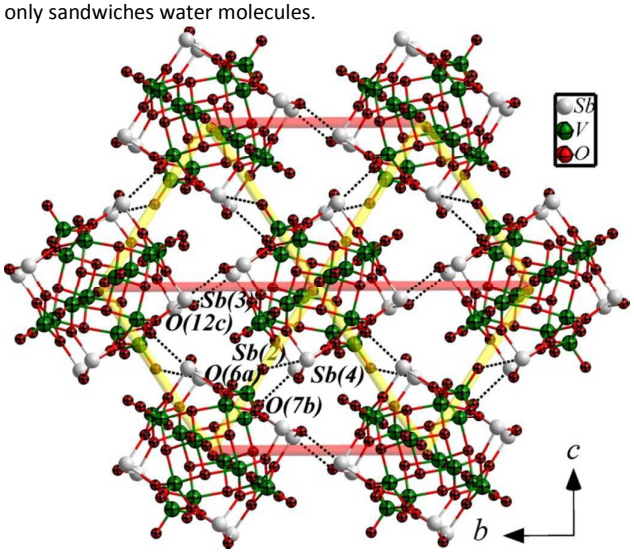

Fig. 6 The 2-D layer structure along the *ac* plane in compound **4**. The red and yellow lines represent the bottom and the two equal length sides of the triangles. Symmetry code: a, -0.5+x, 0.5-y, -0.5+z; b, 1.5-x, 0.5+y, -0.5-z; c, 2-x, 1-y, -z.

Detailed analysis found that there is another important difference between compound **2** and **4**. As shown in Fig. 6, each

$[H_4Sb_8V_{14}O_{42}(H_2O)]$ interacts with six neighboring ones in a hexagonal symmetry into a similar 2-D layer to that of compound **2**. Compared with the 2-D layer in compound **2**, one can found that centroid-centroid distances between each two $[H_4Sb_8V_{14}O_{42}(H_2O)]$ can be divided into two types, one is represented by red line with the centroid-centroid distance of 11.9042(5)Å, the other is represented by yellow line with the distance of 11.463(1)Å (Fig. 6). It should be noted that there are two red lines and four yellow lines around each $[H_4Sb_8V_{14}O_{42}(H_2O)]$, as shown in Fig. 6.

The layers in compound **4** are stacked into a 3-D supramolecular structure. The 3-D supramolecular structure in compound **4** is different from that of compound **2**. Firstly, each two layers in compound **4** did not sandwich TMCs but only some water molecules, and secondly, each unit cell in compound **4** only has one crosscutting layer in it. For there are no TMCs sandwiched between any two inorganic layers of compound **4**, the interplane distance of compound **4** is about 12.69Å, which is shorter than that of compound **2**. There are complex O-H···O hydrogen bonding interactions between different water molecules and water molecules and oxygens from $[H_4Sb_8V_{14}O_{42}(H_2O)]$ with O···O distances in the range of 2.9501(1)-3.1170(3)Å (Table s1), these complex O-H···O hydrogen bonds, together with Sb-O···Sb and V-O···Sb contacts direct POMs in compound **4** into a novel 3-D supramolecular structure.

Structure of compound 5

Single-crystal X-ray diffraction analysis reveals that $[Sb_8V_{14}O_{42}(H_2O)]^{4-}$ in compound **5** is almost the same as $[Sb_8V_{14}O_{42}(H_2O)]^{4-}$ in compound **4** with only slight differences in bond lengths and angles. Bond valence sum calculations suggest that the antimony and vanadium atoms are respectively in +3 and +4 oxidation states.[17]

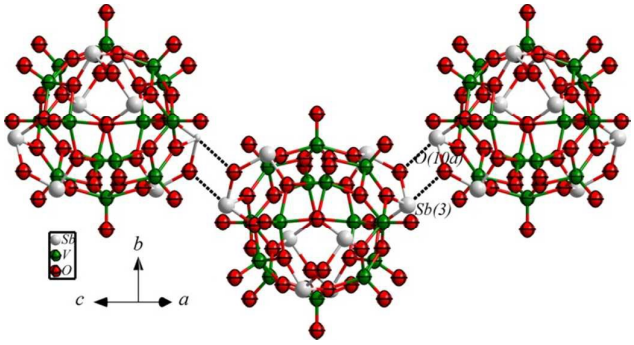

Fig. 7 The 1-D chain structure in compound **5**. Symmetry code: a, -x, 2-y, 1-z.

Compound **5** crystallizes in monoclinic space group C2/*c* with V(5), V(4), O(20), O(14) and O(1w) on a 2-fold rotation axis and all other atoms on general positions. The asymmetric unit is composed of half a $[Sb_8V_{14}O_{42}(H_2O)]^{4-}$, a $[Co(enMe)_3]^{2+}$ and two lattice water molecules. $[Sb_8V_{14}O_{42}(H_2O)]^{4-}$ in compound **5** is not a discrete one but interacts with neighboring $[Sb_8V_{14}O_{42}(H_2O)]^{4-}$ via double Sb-O···Sb contacts with a Sb···O distance of 2.8097(4)Å into a novel 1-D zigzag chain structure along the [*101*] direction. Bensch has reported the compound with a 1-D chain structure $\{Co_2(tren)_3\}_2\{Co(tren)(en)\}[\{V_{15}Sb_6O_{42}(H_2O)(Co(tren)_2)\}V_{15}Sb_6O_{42}(H_2O)]\cdot xH_2O$ (1-D, V-O···Sb, O···Sb distance: 2.88-2.93Å)[12e] based on V-O···Sb contacts. There are some distinctly differences between our compound and Bensch's compound, firstly, the reported compound is based on Sb_6V_{15}, but our compound is based on Sb_8V_{14}. Secondly, the 1-D chain in Bensch's compound is based on V-O···Sb contacts but our compound is based on Sb-O···Sb contacts.

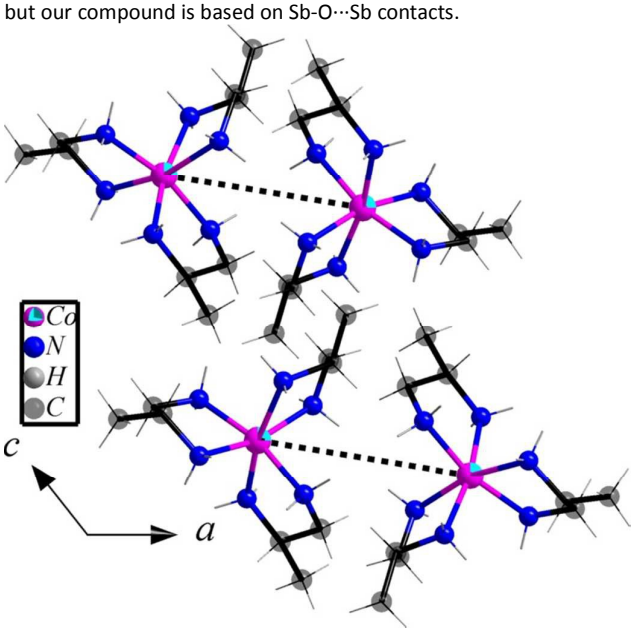

Fig. 8 The left handed screw (Λ) configuration dimer and the right handed screw (Λ) configuration dimer in compound **5**.

Co(1) adopts an octahedral geometry with six nitrogens from three enMe ligands with Co-N distances of 2.145(8)-2.192(7)Å. The crystallographically independent cobalt complex in compound **5** has the left handed screw (Λ) configuration. two symmetry related $[Co(enMe)_3]^{2+}$ with the left handed screw (Λ) configuration was arranged into a dimer with Co-Co distance of 7.6Å, and two symmetry related $[Co(enMe)_3]^{2+}$ with the right handed screw (Λ) configuration was arranged into a dimer with Co-Co distance of 7.6Å, too. It should be noted that there are three right handed screw (Λ) configuration dimers and three left handed screw (Λ) configuration dimers in each unit cell of compound **5**. Therefore, compound **5** crystalize in an achiral space group C2/*c*.

Discussion

Compounds **1**-**3** are based on Sb_6V_{15} clusters and metal-en complexes. Very recently, Schalley and Bensch also reported a series of compounds based on Sb_6V_{15} clusters and metal-en complexes.[18] However, Schalley and Bensch's compounds are very different from our compounds. Firstly, compound **1** is isostructural and isomorphous with Schalley and Bensch's compounds, but compound **1** is based on Cd complexes which is different from Fe, Co or Ni complexes in Schalley and Bensch's compounds; compounds **2** and **3** are thoroughly different from Schalley and Bensch's compounds, both contain two metal-en complexes per formula unit, but Schalley and Bensch's compounds contain three metal-en complexes per formula unit.

Table 2. Structural information for some reported Sb-V compounds.

Compound	Skeleton Structure	Bond type	O···Sb distances
Compound 2	2-D	V-O···Sb	2.77Å
Compound 3	2-D	V-O···Sb	2.77Å
Compound 4	2-D	Sb-O···Sb; V-O···Sb	2.74-2.89Å
$[(enH_2)_2\{Sb_8V_{14}O_{42}(H_2O)\}](en)\cdot 4H_2O$ (**6**)[11b]	1-D	V-O···Sb	2.74-2.79Å
$[C_6H_{17}N_3]_4[Sb_4V_{16}O_{42}]\cdot 2H_2O$ (**7**)[12b]	1-D	V-O···Sb	2.85Å
$(trenH_3)_2[V_{15}Sb_6O_{42}]\cdot 0.33(tren)\cdot nH_2O$ (**8**)[12d]	trimer	Sb-O···Sb	2.88Å
$(enH_2)_2[V_{14}Sb_8O_{42}(H_2O)]\cdot 3H_2O$ (**9**)[12j]	2-D	Sb-O···Sb	2.72, 2.91Å
$(ppzH_2)_2[V_{14}Sb_8O_{42}(H_2O)]$ (**10**) (ppz = piperazine)[12j]	2-D	Sb-O···Sb	2.83, 3.00Å
$[V_{14}Sb_8(C_6N_3H_{15})_4O_{42}(H_2O)]\cdot 4H_2O$ (**11**)[12c]	1-D	Sb-O···Sb	2.73Å
$(Co(N_3C_5H_{15})_2)_2[\{Co(N_3C_5H_{15})_2\}V_{15}Sb_6O_{42}(H_2O)]\cdot 5H_2O$ (**12**)[12h]	dimer	Sb-O···Sb	3.13Å
$\{Ni(C_4N_3H_{13})_2\}_3[V_{15}Sb_6O_{42}(H_2O)]\cdot 2H_2O$ (**13**)[12j]	tetramer	Sb-O···Sb; V-O···Sb	2.67–2.96Å
$\{Co(tren)(H_2O)\}_3[V_{15}Sb_6O_{42}(H_2O)]\cdot H_2O$ (**14**)[12e]	2-D	V-O···Sb	2.90Å
$\{Co_2(tren)_3\}_2\{Co(tren)(en)\}[\{V_{15}Sb_6O_{42}(H_2O)(Co(tren)_2)\}V_{15}Sb_6O_{42}(H_2O)]\cdot xH_2O$ (**15**)[12e]	1-D	V-O···Sb	2.88-2.93Å

The acidity or alkalinity in a synthesis batch is one of the most important parameters for the control of the crystallization of Sb-V compounds. It determines their composition and is to a great extent responsible for the type of the crystallizing product. We have found that the structural type can be influenced by the pH value of the reaction mixtures. The preparation procedures of compounds **1**-**3** are similar. A mixture of Sb_2O_3, NH_4VO_3, H_2O, en and/or DMF should be firstly prepared and stirred for 3h, the alkalinity (pH higher than 10) and the stirring time of the mixture are important for the formation of Sb_6V_{15} clusters in compounds **1**-**3**. The preparation procedure of compound **4** is different from those of compounds **1**-**3**, all the starting materials are mixed together in a short time. The preparation procedure of compound **5** is also unique. A mixture of $CoSO_4$, enMe, H_2O and DMF should be firstly prepared and stirred for 1h, then Sb_2O_3 and NH_4VO_3 was added respectively. In one word, we can conclude that the specific procedures for compounds **1**-**3** play the most important roles in the formation of Sb_6V_{15}-based compounds. However, the relationships between the procedures of compounds **4** and **5** and Sb_8V_{14} compounds are still elusive.

The pH of the final reaction mixture for compound **1** is 10.0, while the pH for final reaction mixtures for compounds **2** and **3** are 8.5 and 9.0, respectively. The acidity for final reaction mixtures for compounds **2** and **3** are higher, resulting in that two extra hydrogen atoms attached on the clusters in the two compounds.

$[Sb_6V_{15}O_{42}(H_2O)]^{6-}$ in compound **1**, containing six negative charges, is discrete. That is to say, there are not intermolecular interactions between $[Sb_6V_{15}O_{42}(H_2O)]^{6-}$ in compound **1**. However, compounds **2** and **4** contain two distinctly different 2-D inorganic layers, of which the layer in compound **2** is formed by $[H_2Sb_6V_{15}O_{42}(H_2O)]^{4-}$ containing four negative charges but the layer in compound **4** is formed by $[H_4Sb_8V_{14}O_{42}(H_2O)]$ which is neutral. In conclusion, there is no proton attached on the cluster of compound **1**, but 2 and 4 protons were attached on the clusters of compounds **2** and **4**, respectively. Protons attached on the clusters of compounds **1**, **2** and **4** are very important for packing structures of the three. When the number of the proton is zero, $[Sb_6V_{15}O_{42}(H_2O)]^{6-}$ in compound **1** has no interactions with other $[Sb_6V_{15}O_{42}(H_2O)]^{6-}$. However, when the number of the protons attached on the cluster is 2, important intermolecular V-O···Sb interactions emerged in compound **2**; and when the number of the protons attached on the cluster is 4, not only V-O···Sb interactions but also Sb-O···Sb interactions emerged in compound **4**.

Compounds containing intermolecular O···Sb interactions have been reported by both Bensch et al. and our group before. However, detailed comparative analysis of the previously reported compounds reveals that the clusters in some of them can also be regarded as protonated ones. We think protons of compounds **6**-**11**[11b, 12b-d, 12j] should be added on surfaces of these clusters.

Bensch also reported compounds **12**-**15**[12e, 12h, 12j] with no protons attached on their clusters. As shown in Table 2, compared the two kinds of O···Sb bond distances, we can concluded that most of O···Sb distances of protonated clusters are relatively shorter, on the contrary, most of O···Sb distances of unprotonated clusters are relatively longer. We think the hydrogen perhaps plays an important role in the formation of the O···Sb interaction: the protonated cluster contains a lower negative charge; therefore, the repulsive force between any two clusters becomes weaker and then the O···Sb distance becomes shorter.

We also found an O···Sb bond between a Sb atom in $[Sb_8V_{14}O_{42}(H_2O)]^{4-}$ and a lattice water molecule with a Sb···O distance of 2.846(2)Å in compound **5**. The difference of IR spectra between compound **1** and compounds **2**-**3** also further demonstrated that there are hydrogen atoms attached on the cluster surfaces of compounds **2**-**3** but not on that of compound **1** (IR spectra part of characterization).

Characterization

In the IR spectrum of compound **1** (Fig. s1), The band at 969cm^{-1} is associated with the terminal V=O stretching vibration, and the strong feature at 713cm^{-1} is ascribed to υ(O-V-O). The patterns of bands in the region characteristic of υ(V=O_t) indicate the presence of V^{IV} sites: clusters which contain exclusively V^{IV} generally possess υ(V=O_t) bands in the range of 970-1000cm^{-1}, while bands in the region 940-960cm^{-1} are characteristic of V^{V}. The observation of a strong absorbance in the 970-1000cm^{-1} region provides a useful

diagnostic for the presence of V^{IV} centers.[19] The multiple strong features in the 1134-1617cm^{-1} region of the IR spectrum of compound **1** are due to vibrations of en ligands in compound **1**.

Both compounds **2** and **3** are based on $[H_2Sb_6V_{15}O_{42}(H_2O)]^{4-}$. It should be noted that the clusters in compounds **2** and **3** should be essentially identical to $[Sb_6V_{15}O_{42}(H_2O)]^{6-}$ in compound **1**. However, compounds **2** and **3** display major different IR spectrum features to that of compound **1**. The IR spectra of compounds **2** and **3** (Fig. s1) show peaks at 957cm^{-1} and 959cm^{-1} corresponding to $\upsilon(V=O_t)$, respectively. 815cm^{-1}, 693cm^{-1} for compound **2** and 717cm^{-1} for compound **3** are respectively due to υ(O-V-O). It is very strange that the band at 815cm^{-1} in the IR spectrum of compound **2** is very strong but not be observed at all in the IR spectra of both compounds **1** and **3**. In addition, the bands corresponding to $\upsilon(V=O_t)$ in compounds **2** and **3** are almost identical, but are distinctly different from that of compound **1**. The difference in their IR spectra of compounds **1**-**3** can be due to the slight difference in their structures and the different attached hydrogen atoms. The IR spectra further demonstrated that there are hydrogen atoms attached to clusters of compounds **2** and **3**.

Compounds **4** and **5** are based on $[Sb_8V_{14}O_{42}(H_2O)]^{4-}$, which is different from those in compounds **1**-**3**. Thus the IR spectra of compounds **4** and **5** are also different from those of compounds **1**-**3**. The bands corresponding to $\upsilon(V-O_t)$ of compounds **4**-**5** are located at 980 and 978cm^{-1}, while the bands associated with υ(O-V-O) of compounds **4** and **5** are located at 694 and 704cm^{-1}. The major difference of the IR spectra of compounds **4** and **5** is that the band at 704cm^{-1} is the strongest one in compound **5** but the band at 624 cm^{-1} is the strongest one in compound **4**. The difference in their IR spectra should also be ascribed to the different attached hydrogen atoms on their POMs.

The powder X-ray diffraction patterns for compounds **1**-**5** are all in good agreement with the ones simulated based on the data of the single-crystal structures, respectively, indicating the purity of the as-synthesized products (Fig. s2). The differences in reflection intensity are probably due to preferential orientations in the powder samples of compounds **1**-**5**.

The UV-Vis spectra of compounds **1-5,** in the range of 250-600nm, are presented in Fig. s3. The UV-Vis spectrum of compound **1** displays an intense absorption sharp peak cantered at about 256nm and tailing to longer wavelengths (to about 450nm), which can be assigned to O→V charge transfer and d→d transitions of complexes in compound **1**. The UV-Vis spectra of compounds **2** and **3** are very similar to that of compound **1**, which displays intense absorption peaks at about 258nm and 257nm assigned to the O→V charge transfer in the polyoxoanion structures of compounds **2** and **3**.[20]

The UV spectra of compounds **4** and **5** are different from those of compounds **1**-**3**, which exhibit absorption peaks at about 277 and 270nm due to the O→V charge transfer in compounds **4** and **5**. The difference of the UV-Vis spectra between compounds **4**-**5** and compounds **1**-**3** can be ascribed to the difference of their clusters.

ESR spectra of compounds **1**-**5** were studied at room temperature (Fig. s4). The ESR spectra of compounds **1**-**5** are very similar to one another, which show Lorentzian shapes accompanied by signals at g=1.98, 2.00, 2.00, 1.96 and 1.95, respectively, indicating that the vanadiums in compounds **1**-**5** are in the in the +4 oxidation state.

Compounds **1**-**3** crystalize in chiral space groups. To explore the chirality of compound **1**-**3**, the solid-stated CD spectra of compounds 1-**3** has been recorded. As shown in Fig. s5, the solid-state CD spectra of compounds **1**-**3** show broad positive cotton effects, indicating the chirality of compounds **1**-**3**.

Table 3. Catalytic activity and product distribution

Catalysts	Styrene conversion (%)	Product selectivity [b] (mol%)		
		So	Bza	Others
Compound **1**	44.0	66.7	31.1	2.2
Compound **2**	18.9	17.7	67.1	15.2
Compound **3**	42.1	20.4	71.9	7.7
Compound **4**	93.0	91.4	7.0	1.6
Compound **5**	29.5	43.1	56.9	0
Compound **6**	77.0	61.0	39.0	0

[b] So: Styrene oxide, Bza: benzaldehyde, Others: including benzoic acid, phenylacetaldehyde. Compound **6** $=[Co(en)_2]_2[Sb_8V_{14}O_{42}(H_2O)]\cdot 6H_2O$.[11a]

The epoxidation of styrene to styrene oxide with aqueous tertbutyl hydroperoxide (TBHP) using compounds **1**-**5** or **6** as a catalyst was carried out in a batch reactor. In a typical run, the catalyst (compound **1** (2mg, 0.6μmol), compound **2** (2mg, 0.7μmol), compound **3** (2mg, 0.7μmol), compound **4** (2mg, 0.8μmol), compound **5** (2mg, 0.7μmol) compound **6** (2mg, 0.8μmol), 0.114ml (1 mmol) of styrene and 2 ml of CH_3CN were added to a 10 ml two-neck flask equipped with a stirrer and a reflux condenser. The mixture was heated to 80°C and then 2 mmol of TBHP was injected into the solution to start the reaction. The liquid organic products were quantified by using a gas chromatograph (Shimadzu, GC-8A) equipped with a flame detector and an HP-5 capillary column and identified by a comparison with authentic samples and GC-MS coupling. The activity of the reaction system to oxidize styrene to styrene oxide in the absence of the catalysts was determined. The result showed that no conversion of the styrene after 8 h.

Table 3 shows the reaction results of TBHP oxidation of styrene over various catalysts at 80ºC. As expected, all the catalysts are active for the TBHP oxidation of styrene. Compound **1** catalyst shows an activity with 44.0% conversion and 66.7% selectivity to styrene oxide after 8h. Nevertheless, Compound **2** shows the lowest activity among the six with 18.9% conversion and 17.7% selectivity to styrene oxide. Compound **3** shows an activity with 42.1% conversion and 20.4% selectivity to styrene oxide. The activity of compound **4** is the highest among the six with 93.0% conversion and the selectivity of compound **4** is 91.4%. The activity and selectivity of compound **5** are 29.5% and 43.1%, respectively, and the activity and selectivity of compound **6** are 77.0% and 61.0%, respectively.

The activity of compound **4** is the highest of the six. The reason comes from its specific structure. As shown in Fig. s6,

the supramolecular structure of compound **4** is formed by pure inorganic layers stacked with only water molecules located between each two neighboring layers. That is to say, the styrene is easy to go into and out of the space between each two neighboring layers (Fig. s6). On the contrary, compounds **2** and **3** have similar inorganic layers to that of compound **4**, however, the space between each two neighboring layers in compounds **2** and **3** are both filled with transition metal complexes. Therefore, the activity of compound **4** is the highest one.

Table 4 Epoxidation catalyzed by different amounts of compound **2**

Catalysts: Compound **2**	Styrene conversion (%)	Product selectivity [b] (mol%)		
		So	Bza	Others
Compound **2**/2mg	18.9	17.7	67.1	15.2
Compound **2**/5mg	79.5	92.6	3.5	4.0
Compound **2**/10mg	88.2	78.3	1.1	20.6
Compound **16**/10mg	91.8	90.9	9.1	0
Compound **17**/10mg	>99	21.2	69.1	9.7
Compound **18**/10mg	54.9	43.8	56.2	0
Compound **19**/10mg	96.2	9.6	82.3	8.1
Compound **20**/10mg	58.7	62.4	37.6	0
Compound **21**/10mg	69.0	59.2	38.3	2.5
Compound **22**/10mg	48.1	51.5	48.5	0
Compound **23**/10mg	83.1	23.1	76.9	0

[b] So: Styrene oxide, Bza: benzaldehyde, Others: including benzoic acid, phenylacetaldehyde. $[Ni(im)(2,2'\text{-bpy})]_2[Ni(im)_2]_2[Ni(2,2'\text{-bpy})][As_8V_{14}O_{42}(H_2O)]$ (**16**), $[Ni(2,2'\text{-bpy})(phen)][Ni(2,2'\text{-bpy})_2][As_8V_{14}O_{42}(H_2O)]\cdot H_2O$ (**17**), $[Ni(2,2'\text{-biim})(2,2'\text{-bpy})_2]_2[As_8V_{14}O_{42}(H_2O)]\cdot 6H_2O$ (**18**) $[Cd(2,2'\text{-bpy})(phen)_2]_2[As_8V_{14}O_{42}(H_2O)]\cdot 4H_2O$ (**19**), $[Cd_4(phen)_4(ox)(H_2O)_6][As_6V_{15}O_{42}(H_2O)]\cdot 2H_2O$ (**20**), $[Co_2(phen)_4(ox)][H_2As_8V_{14}O_{42}(H_2O)]\cdot(apy)_2\cdot 2H_2O$ (**21**), $[As_8V_{14}O_{42}(H_2O)][Cd(1,10\text{-Phen})_3]_2$ (**22**), $[As_8V_{14}O_{42}(H_2O)][Ni(2,2'\text{-biim})_3]_2\cdot 6H_2O$, (Him=Imidazole, phen =1, 10-phenanthroline, 2,2'-biim=2,2'-biimidazole, apy = 2-aminopyridine)[5i, 21]

Compound **2** shows the lowest activity and selectivity among the six. But very fortunately, we have synthesized enough crystals of compound **2**. Thus the same experimental conditions were used except that 5mg or 10mg of compound **2** was used as catalyst. It was found that with the increase of the amount of compound **2**, both the activity and selectivity increased obviously (Table 4): when the catalyst is 5mg, the conversion is 79.5% and the selectivity is 92.6%; by contrast, when the catalyst is 10mg, the conversion is 88.2% and the selectivity is 78.3%. It is clear that with the increase in the amount of compound **2**, the conversion of styrene increased. However, when the amount of compound **2** is increased from 5mg to 10mg, the selectivity decreased from 92.6% to 78.3%. It should be noted that such phenomenon is commonly seen in catalytic reactions.[22]

We have already carried out identical catalytic experiments previously by only using As-V analogous compounds replacing Sb-V compounds as catalysts, and from these experiments we found that Sb-V compounds are more efficient than As-V analogies for epoxidation of styrene (Table 4). The amount of the As-V catalysts used was 10mg, but the amount of the Sb-V catalysts was only 2mg. Even compound **2** with the lowest conversion shows a relatively high conversion when the amount of compound **2** is increased to 10mg compared with any As-V catalyst.

Conclusion

Five new self-assembly hybrid compounds based on Sb-V clusters have been synthesized and characterized. Compound **1** is a chiral compound constructed from $[Sb_6V_{15}O_{42}(H_2O)]^{6-}$ (Sb_6V_{15}) and $[Cd(en)_3]^{2+}$. Compounds **2** and **3** are isostructural and isomorphous. Each of the two contains a 2-D inorganic layer formed by $[H_2Sb_6V_{15}O_{42}(H_2O)]^{4-}$ via V-O···Sb contacts. Compound **4** contains a 2-D inorganic layer formed by $[H_4Sb_8V_{14}O_{42}(H_2O)]$ via both V-O···Sb and Sb-O···Sb interactions. Compound **5** contains a 1-D zigzag chain structure formed by $[Sb_8V_{14}O_{42}(H_2O)]^{4-}$ (Sb_8V_{14}) via Sb-O···Sb contacts. The catalytic properties of compounds **1**-**5** have been done and we found that compounds **1**-**5** can be used as efficient catalysts for the epoxidation reaction of styrene to styrene oxide.

Acknowledgements

This work was supported by National Natural Science Foundation of China under Grant No. 21003056 and supported by Key Laboratory of Functional Inorganic Material Chemistry (Heilongjiang University), Ministry of Education.

Notes and references

‡ Footnotes relating to the main text should appear here. These might include comments relevant to but not central to the matter under discussion, limited experimental and spectral data, and crystallographic data.
§
§§
etc.

1. a) M. T. Pope, *Heteropoly and Isopoly Oxometalates*, Springer, Berlin, 1983; b) M. T. Pope and A. Müller, *Angew. Chem., Int. Edit. Engl.*, 1991, **30**, 34; c) M. T. Pope and A. Müller, *Polyoxometalates: From Platonic Solids to Anti-Retro Viral Activity*, Kluwer, Dordrecht, The Netherlands, 1994; d) T. Yamase and M. T. Pope, *Polyoxometalate Chemistry for Nano-Composite Design*, the Netherlands, Kluwer, Dordrecht, 2002; e) D. L. Long, E. Burkholder and L. Cronin, *Chem. Soc. Rev.*, 2007, 105; f) D. L. Long, R. Tsunashima and L. Cronin, *Angew. Chem. Int. Ed. Engl.*, 2010, **49**, 1736; g) H. M. Miras, L. Vila-Nadal and L. Cronin, *Chem. Soc. Rev.*, 2014, **43**, 5679; h) A. Proust, R. Thouvenot and P. Gouzerh, *Chem. Commun.*, 2008, 1837; i) A. Proust, B. Matt, R. Villanneau, G. Guillemot and G. L. P. Guozerh, *Chem. Soc. Rev.*, 2012, **41**, 7605; j) A. Dolbecq, E. Dumas, C. R. Mayer and P. Mialane, *Chem. Rev.*, 2010, **110**, 6009; k) S. Roy, *CrystEngComm.*, 2014, **16**, 4667.

2. a) J. Berzelius, *Poggendorff's, Ann. Phys.*, 1826, **6**, 369; b) J. F. Keggin, *Nature*, 1933, **131**, 908.
3. I. M. Mbomekalle, R. Cao, K. I. Hardcastle, C. L. Hil, M. Ammam, B. Keita, L. Nadjo and T. M. Anderson, *C. R. Chimie*, 2005, **8**, 1077.
4. a) A. Müller and J. Döring, *Angew. Chem. Int. Ed. Engl.*, 1988, **27**, 1721; b) G. Huan, M. A. Greaney and A. J. Jacobson, *j. Chem. Soc., Chem. Commun.*, 1991, 260; c) R. Basler, G. Chaboussant, A. Sieber, H. Andres, M. Murrie, P. Kögerler, H. Bögge, D. C. Crans, E. Krickemeyer, S. Janssen, H. Mutka, A. Müller and H. U. Gudel, *Inorg. Chem.*, 2002, **41**, 5675.
5. a) X. B. Cui, J. Q. Xu, Y. Li, Y. H. Sun and G. Y. Yang, *Eur. J. Inorg. Chem.*, 2004, 1051; b) X. B. Cui, J. Q. Xu, H. Meng, S. T. Zheng and G. Y. Yang, *Inorg. Chem.*, 2004, **43**, 8005; c) X. B. Cui, Y. Q. Sun and G. Y. Yang, *Inorg. Chem. Commun.*, 2003, **6**, 259; d) X. B. Cui, J. Q. Xu, L. Ding, H. Ding, L. Ye and G. Y. Yang, *J. Mol. Struct.*, 2003, **660**, 131; e) X. B. Cui, J. Q. Xu, Y. Li, Y. H. Sun, L. Ye and G. Y. Yang, *J. Mol. Struct.*, 2003, **657**, 397; f) X. B. Cui, J. Q. Xu, Y. H. Sun, Y. Li, L. Ye and G. Y. Yang, *Inorg. Chem. Commun.*, 2004, **7**, 58; g) X. B. Cui, K. C. Li, L. Ye, Y. Chen, J. Q. Xu, W. J. Duan, H. H. Yu, Z. H. Yi and J. W. Cui, *J. Solid. State. Chem*, 2008, **181**, 221; h) S. Y. Shi, Y. Chen, J. N. Xu, Y. C. Zou, X. B. Cui, Y. Wang, T. G. Wang, J. Q. Xu and Z. M. Gao, *CrystEngComm.*, 2010, **12**, 1949; i) H. Y. Guo, Z. F. Li, D. C. Zhao, Y. Y. Hu, L. N. Xiao, X. B. Cui, J. Q. Guan and J. Q. Xu, *CrystEngComm.*, 2014, **16**, 2251.
6. J. Do and A. J. Jacobson, *Inorg. Chem.*, 2001, **40**, 2468.
7. J. Spengler, F. Anderle, E. Bosch, P. K. Grasselli, B. Pillep, P. Behrens, O. P. Lapina, A. A. Shubin, H.-J. Eberle and H. Knözinger, *J. Phys. Chem. B.*, 2001, **105**, 10772.
8. M. I. Khan, S. Tabussum, C. L. Marshall and M. K. Neylon, *catal. Lett.*, 2006, **112**, 1.
9. S. Albonetti, F. Cavani, F. Trifiro, M. Gazzano, F. C. Aissi, A. Aboukais and M. J. Guelton, *j. Catal.*, 1994, **146**, 491.
10. F. Cavani, A. Tanguy, F. Trifiro and M. Koutrev, *J. Catal.*, 1998, **174**, 231.
11. a) L. J. Zhang, X. L. Zhao, J. Q. Xu and T. G. Wang, *J. Chem. Soc., Dalton Trans.*, 2002, 3275; b) X. X. Hu, J. Q. Xu, X. B. Cui, J. F. Song and T. G. Wang, *inorg. Chem. Commun.*, 2004, **7**, 264.
12. a) H. Lühmann, C. Näther, P. Kögerler and W. Bensch, *Inorg. Chim. Acta.*, 2014, **421**, 549; b) R. Kiebach, C. Näther and W. Bensch, *Solid. State. Sci.*, 2006, **8**, 964; c) E. Antonova, C. Näther, P. Kögerler and W. Bensch, *angew. Chem. Int. Ed.*, 2011, **50**, 764; d) R. Kiebach, C. Näther, P. Kögerler and W. Bensch, *Dalton Trans.*, 2007, 3221; e) E. Antonova, C. Näther and W. Bensch, *CrystEngComm.*, 2012, **14**, 6853; f) E. Antonova, C. Näther, P. Kögerler and W. Bensch, *Dalton Trans.*, 2012, **41**, 6957; g) A. Wutkowski, C. Näther, P. Kögerler and W. Bensch, *Inorg. Chem.*, 2008, **47**, 1916; h) E. Antonova, C. Näther, P. Kögerler and W. Bensch, *Inorg. Chem.*, 2012, **51**, 2311; i) E. Antonova, C. Näther and W. Bensch, *Dalton Trans.*, 2012, **41**, 1338; j) E. Antonova, A. Wutkowski, C. Näther and W. Bensch, *Solid. State. Sci.*, 2011, **13**, 2154; k) A. Wutkowski, C. Näther, P. Kögerler and W. Bensch, *Inorg. Chem.*, 2013, **52**, 3280-3284; l) Y. Li, J. P. Liu, J. P. Wang and J. Y. Niu, *Chem. Res. Chin. Univ.*, 2009, **25**, 426; m) Y. Z. Gao, Z. G. Han, Y. Q. Xu and C. W. Hu, *J. Cluster. Sci.*, 2010, **21**, 163.
13. K. Y. Monakhov., W. Bensch. and P. Kögerler, *Chem. Soc. Rev.*, 2015, **44**, 8443.
14. P. J. Hagraman and J. Zubieta, *Inorg. Chem.*, 2000, **39**, 3252.
15. G. Sheldrick, *Acta Crystallogr., Sec. A.*, 2008, **64**, 112.
16. L. Farrugia, *J. Appl. Crystallogr.*, 2012, **45**, 849.
17. I. D. Brown, *in Structure and Bonding in Crystals, edited by M. O'Keefe, A. Navrotsky*, Academic Press, New York, 1981.
18. M. Wendt, U. Warzok, C. Näther, J. V. Leusen, P. Kögerler, C. A. Schalley and W. Bensch, *Chem. Sci.*, 2015, **DOI: 10.1039/C5SC04571A**.
19. T. D. Keene, D. M. D'Alessandro, K. W. Krämer, J. R. Price, D. J. Price, S. Decurtins and C. J. Kepert, *Inorg. Chem.*, 2012, **51**, 9192.
20. H. J. Tian, I. E. Wachs and L. E. Briand, *J. Phys. Chem. B.*, 2005, **109**, 23491.
21. H. Y. Guo, Z. F. Li, X. Zhang, L. W. Fu, Y. Y. Hu, L. L. Guo, X. B. Cui, Q. S. Huo and J. Q. Xu, *CrystEngComm.*, 2016, **18**, 566.
22. a) Y. Nakagawa, R. Tamura, M. Tamura and K. Tomishige, *Sci. Technol. Adv. Mater.*, 2015, **16**, 014901; b) H. L. Gao, H. T. Liu, B. Pang, G. Yu, J. Du, Y. D. Zhang, H. S. Wang and X. D. Mu, *Bioresource Technol.*, 2014, **172**, 453.